Observations of Near-Earth Asteroid 2010 CN141 with the Wide-field Infrared Survey Explorer (WISE)

Sean Marshall

Sean.E.Marshall@asu.edu

School of Earth and Space Exploration, Arizona State University, PO Box 871404, Tempe, AZ 85287-1404

UCLA Astronomy, PO Box 951547, Los Angeles, CA 90095-1547

ABSTRACT

The near-Earth asteroid 2010 CN141 was discovered by WISE in February 2010, with follow-up observations from Mauna Kea from February to April. Its low visual albedo and its proximity to Earth caught the attention of observers, and it was selected for more detailed analysis. Its orbit brought it back into WISE's field of view in May, though it was near WISE's detection limit, and it was uncertain whether the asteroid would actually be visible. Subsequent analysis revealed a faint spot inside the error ellipse that was probably but not conclusively 2010 CN141. The spot was about three arcseconds from the asteroid's expected position. Thermal modeling of the February observations indicates that the asteroid has a diameter of 287 ± 34 m, a visual geometric albedo of 0.0252 ± 0.0065, and a bolometric Bond albedo of 0.0099 ± 0.0025.

1. INTRODUCTION

NASA's Wide-field Infrared Survey Explorer (WISE) was launched on December 14, 2009. Its overall goal is to survey the entire sky in the infrared. It has four channels, which are centered at 3.4, 4.6, 12, and 22 μm. WISE's primary mirror has a diameter of 40 cm. Its field of view is 47 arcminutes. WISE has a resolution of about 6 arcseconds in bands 1-3 and about 12 arcseconds in band 4 (Wright et al. 2010).

WISE is in a Sun synchronous orbit around the Earth, with a sub-spacecraft local solar time of 6 AM or 6 PM. It is always looking about ninety degrees away from the Sun (Wright 2010). WISE's scan pattern typically allows it to capture about two dozen images of any solar system object within a period of about two days. After that, the object is out of WISE's field of view. Therefore WISE is quite capable of seeing the motion of a solar system object, but any newly discovered bodies must be subsequently observed within about two weeks. Without subsequent observations, the object is effectively lost, due to uncertainty in its orbit.

2010 CN141, also known by the shortened designation K10CE1N, was first observed by WISE from February 13 to February 15, 2010 (Spahr 2010). Follow-up observations from Mauna Kea by M. Micheli, G. T. Elliott, and D. J. Tholen on February 21 and March 24 allowed for the determination of a much more accurate orbit (MPC 2010a). The asteroid's orbit has a semimajor axis of 1.516 AU, quite similar to that of Mars. However, its orbit is much more eccentric, giving it a perihelion distance of 0.9114 AU. It is therefore an Earth-crossing Apollo-class asteroid (Yeomans 2010). Fortunately, its orbit is significantly inclined (23.81 degrees) with respect to the ecliptic, giving it a minimum orbit intersection distance (MOID) with respect to Earth of 0.06 AU, about 23 times greater than the distance from Earth to the Moon. 2010 CN141 was originally calculated to have an Earth MOID of 0.04 AU (Spahr 2010), below the

threshold of 0.05 AU defined for potentially hazardous asteroids, but the improved orbit means that it is no longer considered a PHA.

The Mauna Kea team also observed the asteroid on April 5, 2010 (MPC 2010b). However, that observation was not reported until after this report was nearly complete, and most of the computations here were done without incorporating information from that final observation.

2. SEARCH PROCEDURE

The geometry of 2010 CN141's orbit and WISE's scan pattern brought it back into WISE's field of view in mid May. At that time, the asteroid was more than twice as far from the Earth as it was during the February observations, and as such, it was expected to be near WISE's detection limit. As a further complication, growing uncertainty in the asteroid's position meant that it had a three-sigma error ellipse that was 2.6 arcminutes by 0.3 arcminutes, which in WISE W3 pixels is 58 × 6.

2010 CN141 is not obviously visible in the May frames, but careful processing and stacking of the proper frames were attempted, in order to look more carefully. Only frames from band W3 (centered at about 12 μm) were analyzed, as that band contains the asteroid's expected thermal emission peak. Analysis was done using IDL.

The first step was the compilation of the list of WISE W3 frames expected to contain 2010 CN141 within their field of view, as well as relevant parameters like the asteroid's position and the associated uncertainty.

The azimuthally averaged WISE W3 point-spread function (PSF) resembles a Gaussian but has slightly larger values in its "tail" (see Wright et al. 2010, Figure 11). Its form was analyzed and used as the basis for data fitting.

For each frame, a set of pseudo-Gaussians were fit to each pixel in a region containing the error ellipse. The pseudo-Gaussian PSF values were simply interpolated from a tabulated set of values of the W3 PSF (Wright et al. 2010). The fits had the form

$$z(r) = B + F \times \mathrm{psf}(r) \tag{1}$$

where B is the background, F is the amplitude of the object's flux, and r is the radial distance from the PSF's center. The PSF values only had to be calculated once. Given the form of the point-spread function and the WISE observations' data values, linear least squares fitting was performed on the data.

For each pixel in the region, a pseudo-Gaussian was fit that was constrained to be centered at each pixel. The important fit parameter is F. Clearly, a large positive value of F indicates the presence of a bright source at (or near) that pixel, and a value that is negative (or close to zero) indicates that there is not a bright source.

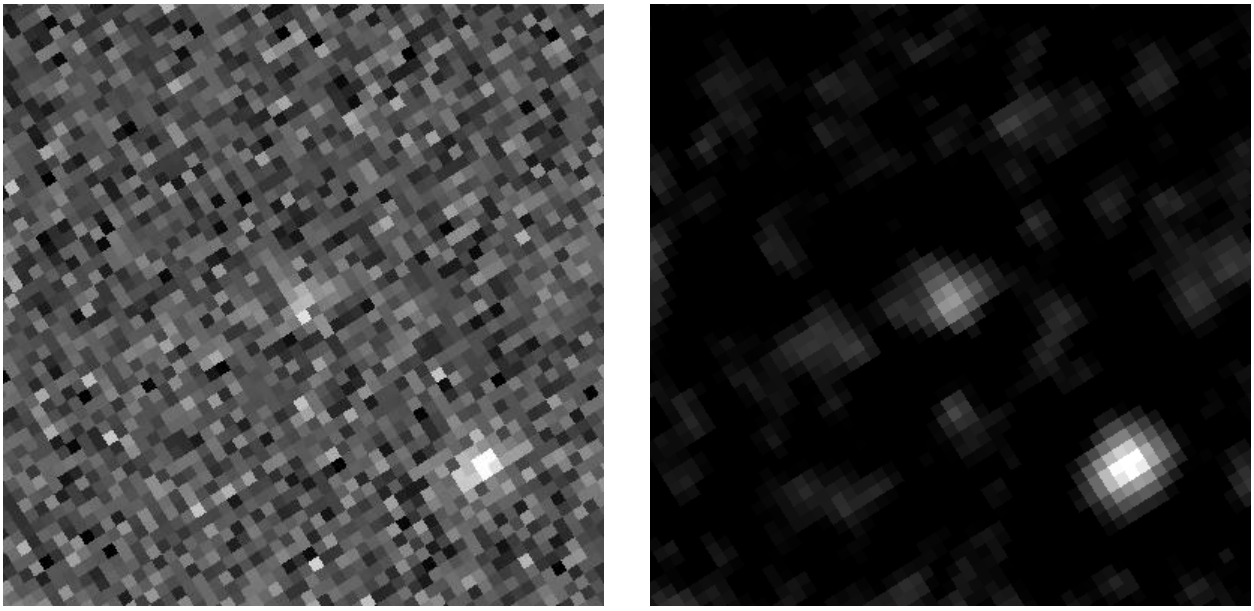

Fig. 1.– Pseudo-Gaussian fits to WISE frame 01878a249 W3. On the left are the data, as acquired by WISE on February 14, 2010. On the right are the fitted fluxes to the same subregion of the same frame. In all WISE data (and fitted fluxes) shown in this document, 2010 CN141 is at the center, and north is up. Note that the asteroid is much more noticeable in the fitted flux image. Both images use linear scaling. The left image shows any data four (or more) median absolute deviations (MAD's) below the median as black and any data eight (or more) MAD's above the median as white. Median and MAD were used because they are more robust than mean and standard deviation. In the right image, black represents any pixel with a fitted flux of zero (or negative) DN, and white represents 150 (or more) DN. For comparison, the background was typically about 1200 DN, and MAD was usually about one fourth of standard deviation.

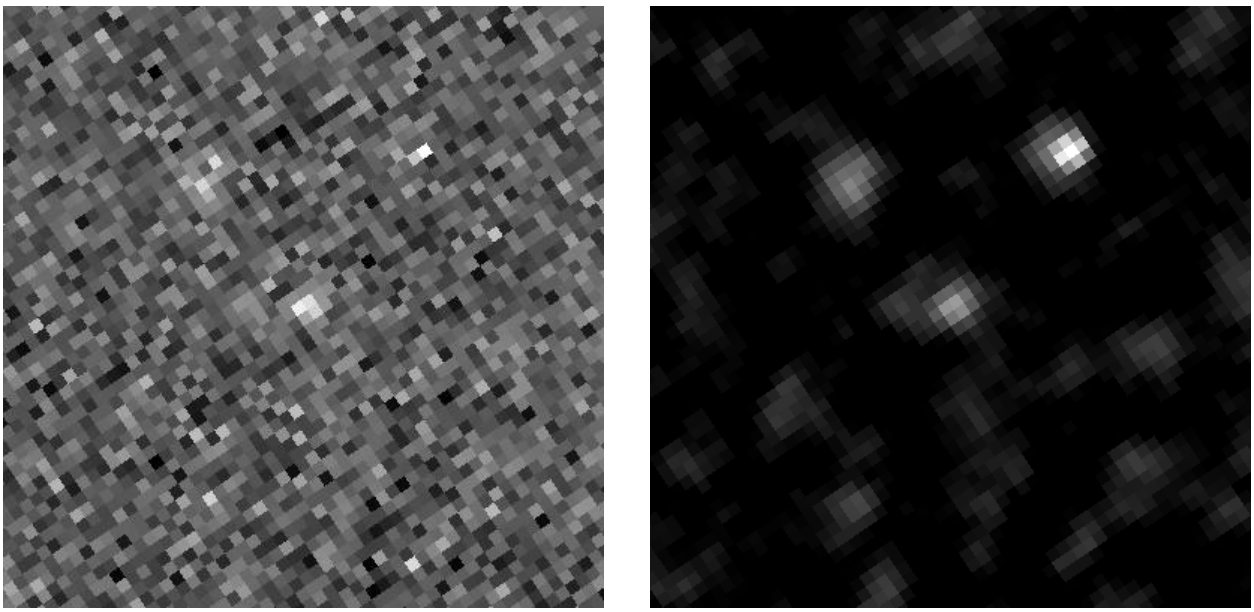

Fig. 2.– Pseudo-Gaussian fits to frame 01910a248 W3. The data, acquired on February 15, 2010, are on the left, and fitted fluxes are on the right. Images are scaled in the same manner as Fig. 1.

Figures 1 and 2 show that the fitted fluxes work well for bringing out bright sources, effectively filtering the images. Taking an average over a set of frames is even more effective at isolating the solar system object of interest.

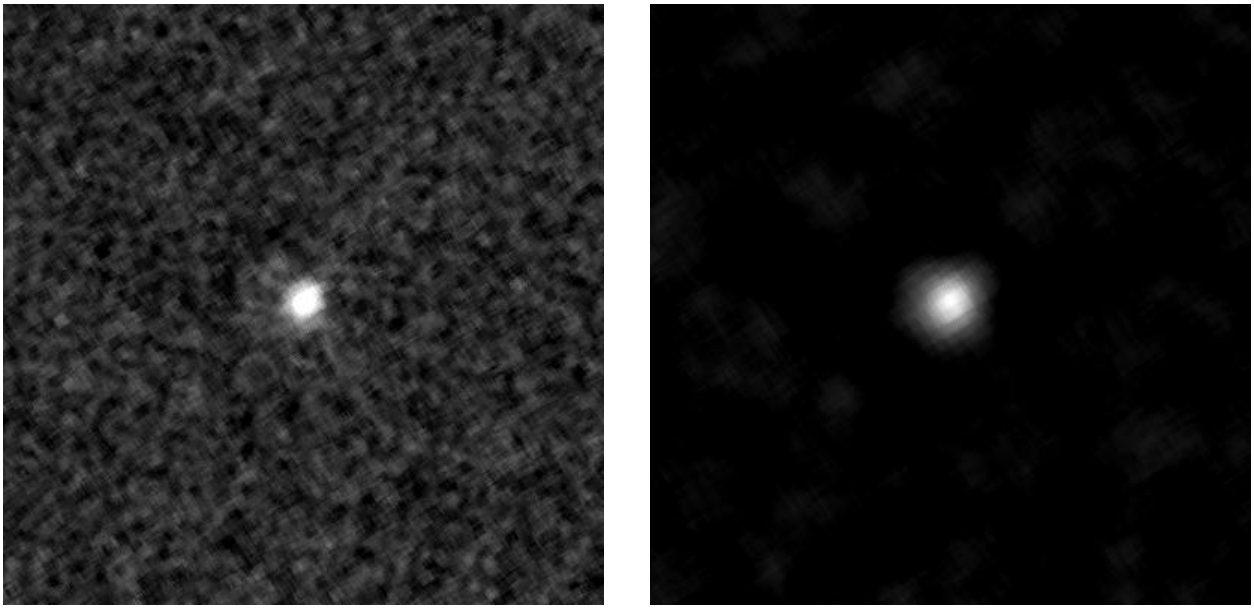

Fig. 3.– Mid-means (means of data between first and third quartiles) of the WISE frames from February 2010 showing 2010 CN141. The left image shows the mid-means of the WISE DN values, and the right image shows the mid-means of the fitted fluxes. These images were generated by stacking subsections of the individual frames, with each subsection centered on 2010 CN141, magnified, and rotated to have north at the top. 2010 CN141 is the only source in those 25 frames that is consistently bright with respect to its (time-varying) position, as one would expect. Both images use linear scaling. On the left, black is four (or more) MAD's below the median normalized DN. White is twenty (or more) MAD's above the median, which is roughly equal to five standard deviations above the mean. On the right, black represents a fitted flux of zero (or negative), and white represents a fitted flux of 91.75 DN (the maximum value).

3. SEARCH RESULTS

The pseudo-Gaussian fitting procedure was then applied to the later frames containing 2010 CN141 within their field of view, which were acquired from May 10 through May 13. Since that time range (less than three days) is small compared to the time since the last observation (47 days), it was reasoned that if 2010 CN141 is not at its expected position, as calculated from the previously determined orbit, it should be offset by the same amount in each of the May frames. For instance, if it is five arcseconds south of the expected position in one frame, it should be about five arcseconds south of the expected position in all of the May frames.

Applying the procedure to individual frames from May, where 2010 CN141 is near the detection limit but its error ellipse is within the frames, yields inconclusive results.

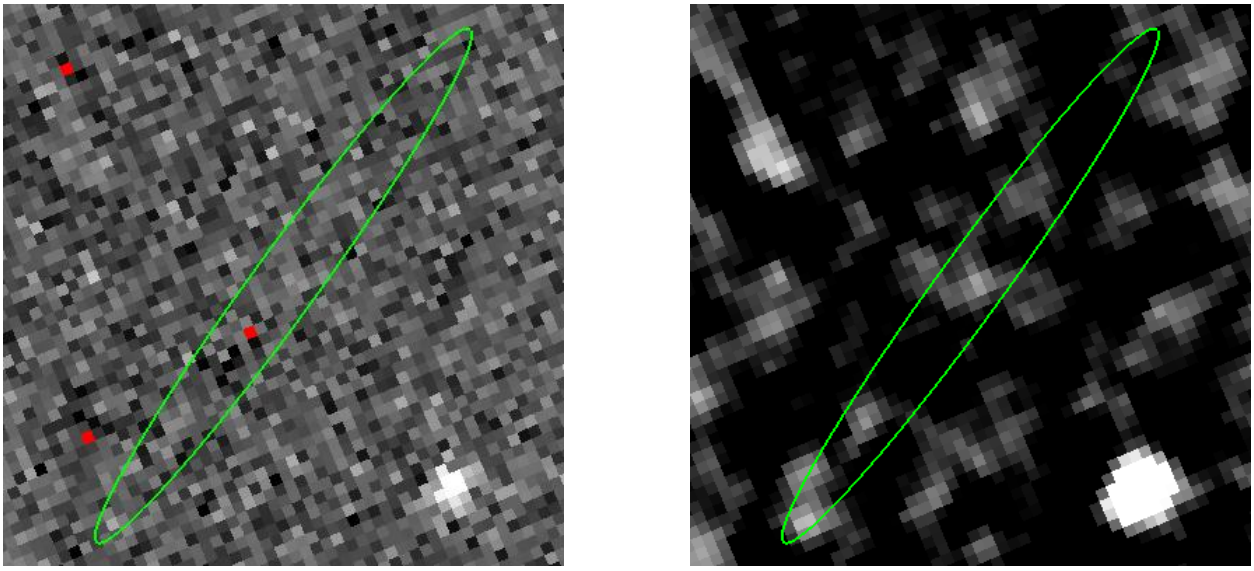

Fig. 4.– Pseudo-Gaussian fits to WISE frame 04513a155 W3. As before, the data, acquired on May 12, 2010, are on the left, and the fitted fluxes are on the right. The three-sigma error ellipse is shown in green. Red indicates invalid pixels, which were omitted from the fit calculations. The fitted fluxes for this frame seem encouraging, as there are several fairly bright spots within the error ellipse, but none of those bright spots is consistently present in the other May frames. Data are scaled as in Figures 1 and 2, except that white regions in the right image represent a fitted flux of (at least) 60 DN, instead of 150.

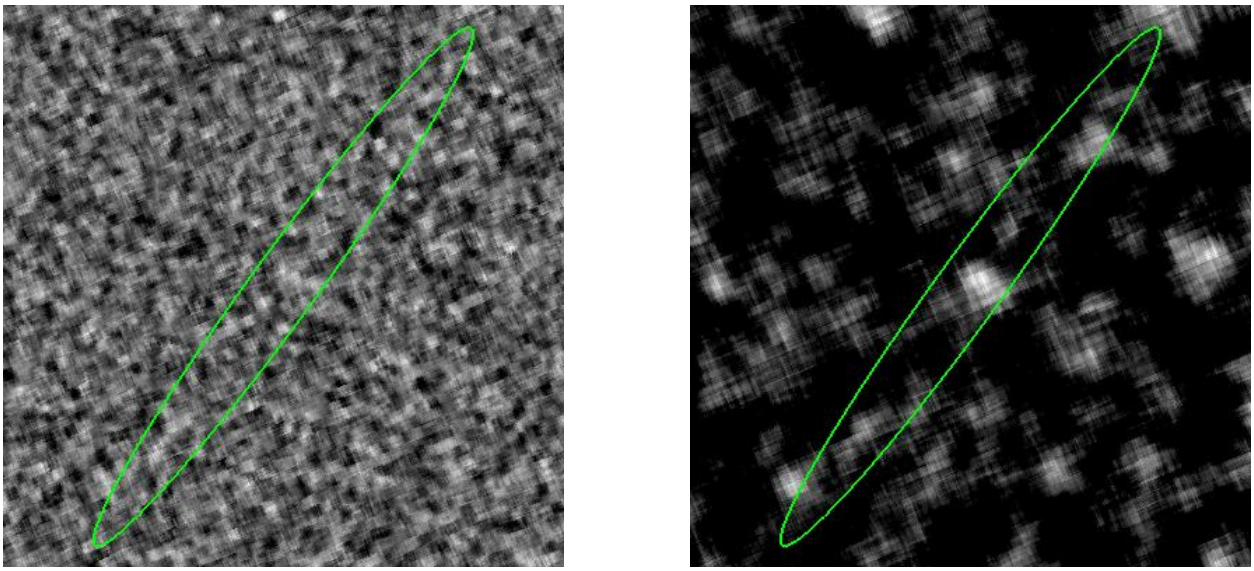

Fig. 5.– Mid-means of 28 frames from May 2010, centered with respect to 2010 CN141's expected position. As before, the data are on the left, and the fitted fluxes are on the right. The three-sigma error ellipse is shown in green. There are no bright spots that stand out above the noise in the data. In the fitted fluxes, however, there is a relatively bright spot close to the center of the error ellipse. Both images are scaled linearly. On the left, black represents a mid-mean normalized DN four (or more) MAD's below the median, and white represents 6.68 MAD's (the maximum) above the median. On the right, black represents a fitted flux of zero or less DN, and white represents 11.8 DN (the maximum).

Averaging over the May frames is more promising. Figure 5 shows a spot with relatively high mid-mean fitted flux near the center of the error ellipse. This is not a peculiarity of the mid-mean; a spot is seen at the same location in similarly computed images of the mean and median fitted fluxes. The spot is about three arcseconds to the west and one arcsecond to the north of 2010 CN141's expected position. Its average fitted flux is 10 ± 3 WISE DN.

However, while the fitted flux at that offset is relatively high on average (the spot was analyzed for that reason), it is not consistent. At that location, some frames have a negative value for the fitted flux, and as seen in Figure 6, most of the fitted fluxes' error bars contain zero.

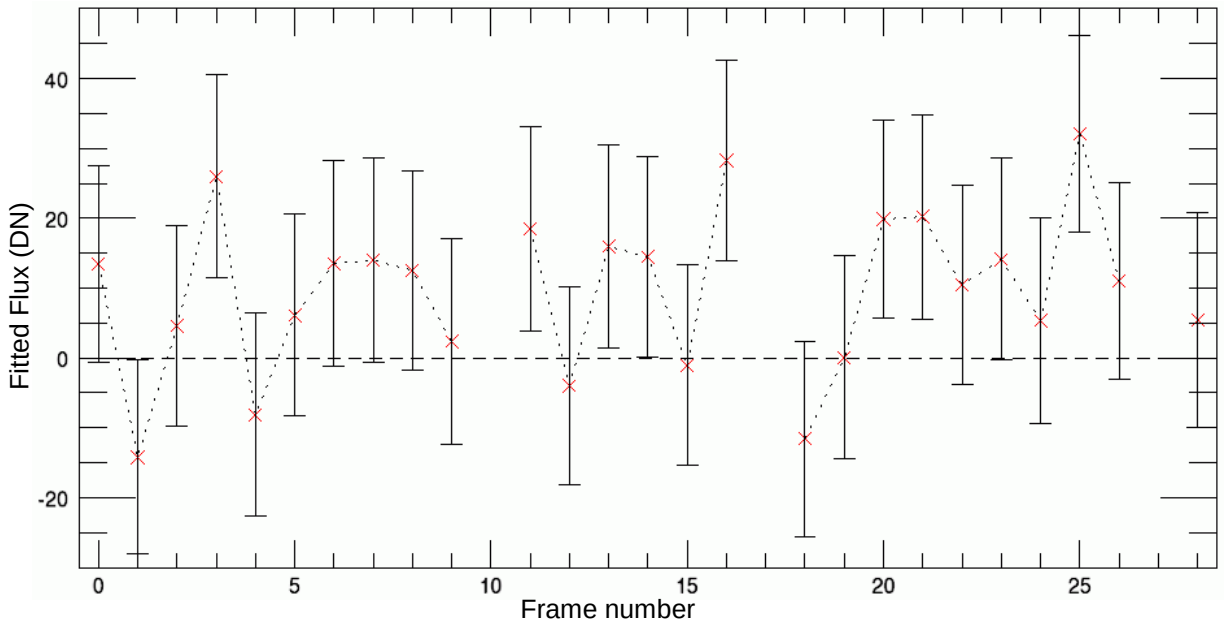

Fig. 6.– Fitted flux at the bright spot in the May frames (values in WISE DN). Even at the brightest spot in the error ellipse, the fitted fluxes are not consistently positive. Gaps are due to the spot being outside the image boundaries of some frames.

4. FUTURE OBSERVATIONS

The May frames are probably correct, but it will only be possible to confirm or deny the detection of 2010 CN141 after future observations can be used to calculate a more accurate orbit, and it will be possible to check whether the bright spot's position is consistent with that orbit.

WISE will almost certainly be out of coolant before it would have another chance to see the asteroid. However, during the fall of 2011, at about the time of 2010 CN141's next perihelion passage, it will be relatively close to Earth, so there will be good opportunities then.

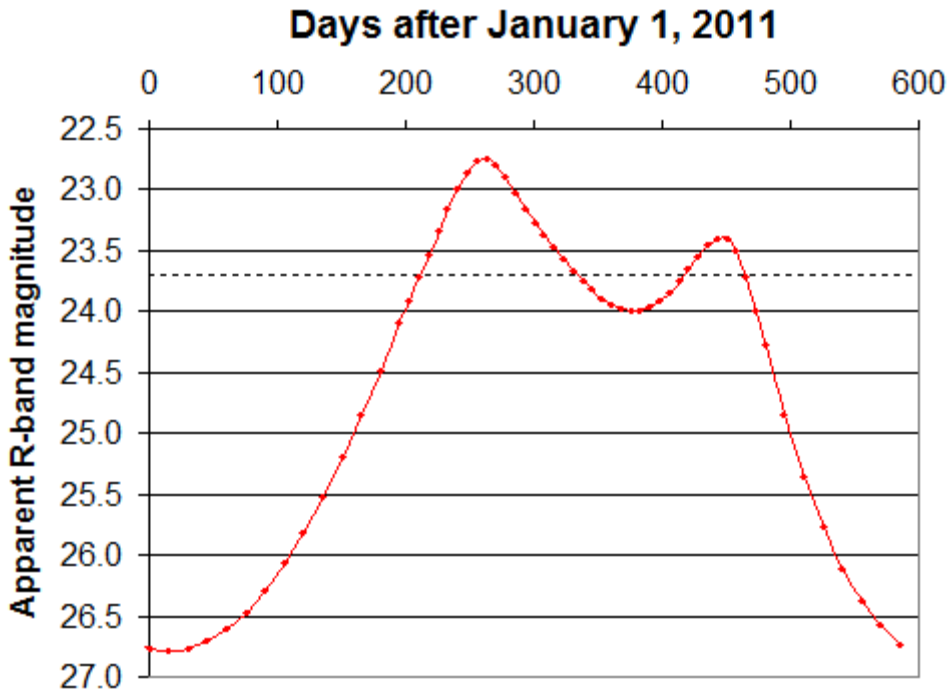

Fig. 7.– Expected apparent R-band magnitude of 2010 CN141 in 2011 and 2012. The dotted line is m_R = 23.7, the faintest magnitude at which it has been observed in that band from Mauna Kea.

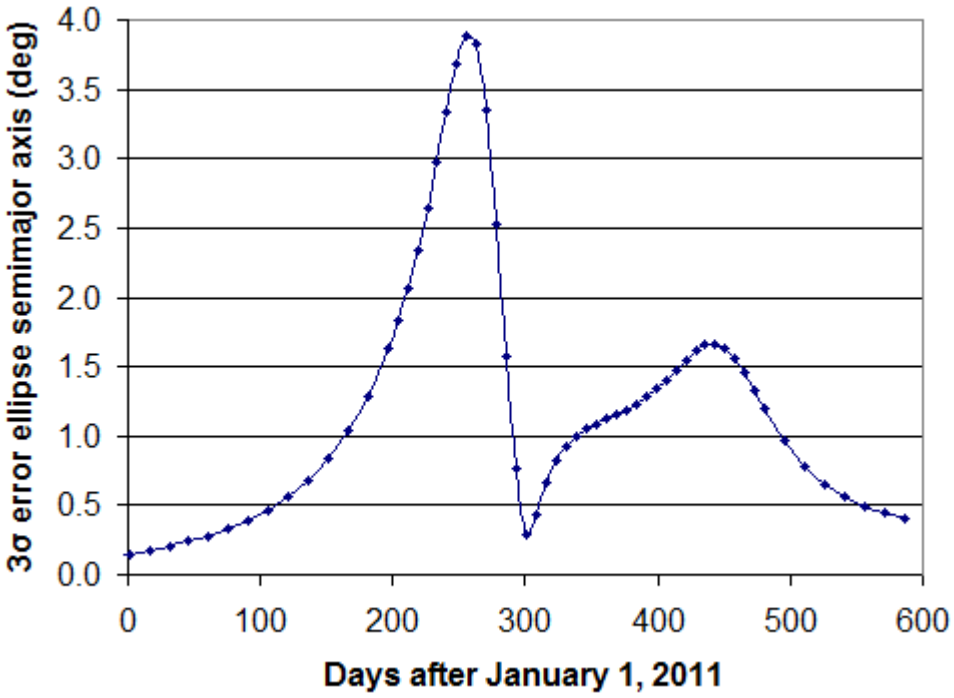

Fig. 8.– Uncertainty in position of 2010 CN141 in 2011 and 2012. The plotted value is the length of the three-sigma semimajor axis. The semiminor axis is usually shorter by two (or more) orders of magnitude. The rapid decrease before day 300 is due to orbital geometry. These values are based on an ephemeris that incorporates the April observation from Mauna Kea.

Figure 7 shows that 2010 CN141 will be bright enough to be detected for a while in late 2011 and early 2012. Figure 8 shows the uncertainty in the asteroid's position for the same range of times, based on its orbit as determined from the observations in February and March. It will be easiest to find at about day 300 (October 28) of 2011. At that time, 2010 CN141 is close to perihelion, and observers on Earth will be looking almost exactly along its velocity vector; thus, at that time there will be relatively little uncertainty in its coordinates. Observations at a different time would allow for a more accurate determination of 2010 CN141's orbit, if it can be found, as they would be reducing the positional uncertainty by a greater factor. However, observations at any time would be highly valuable. It may be easiest to find the asteroid when it is close to perihelion, and then to continue to track it.

5. THERMAL MODELING

The data from the February observations of 2010 CN141, when processed with simple thermal models, allow the estimation of some of its important physical properties: diameter, visual geometric albedo, and bolometric Bond albedo.

Visual geometric albedo (p_v) is the proportion of radiation in the visible band (about 550 nm) that is reflected by a body. Bond albedo (A) is the fraction of all incident solar radiation (at all wavelengths) that is reflected by a body. The two are related by

$$A = qp_v \tag{2}$$

where q is the phase integral for the asteroid (Harris and Lagerros 2002). The phase integral can be calculated from the asteroid's magnitude slope parameter (G) as

$$q = 0.290 + 0.684G \tag{3}$$

In general, one divides the visible half of the asteroid into many subregions, uses a thermal model to calculate the temperature of each subregion, assumes that each subregion is a blackbody, calculates its flux at a given wavelength (presumably the wavelength being observed), and then adds up the contributions from each subregion to find the asteroid's total flux at that wavelength. Each thermal model has its basis in the assumption that the power emitted from a given point on the asteroid is in some sort of equilibrium with the incident solar flux.

The standard thermal model (STM) assumes that every point on an asteroid (which is assumed to be a smooth sphere) has a temperature such that the power it radiates through thermal emission is exactly equal to the instantaneous power incident upon it from the Sun. Therefore the temperature of a point depends only on "the angular distance from the subsolar point", or, equivalently, the local solar incidence angle (Harris and Lagerros 2002). This is a reasonable assumption for asteroids with slow rotation and low thermal inertia. The subsolar point has the highest temperature:

$$T_0 = \sqrt[4]{\frac{(1-A)F}{\eta\varepsilon\sigma}} \tag{4}$$

where A is the Bond albedo, F is the solar flux at the asteroid's position (equal to the Sun's luminosity divided by $4\pi d^2$), η is a normalization parameter to account for the effects of beaming at low phase angles (it is assumed to equal 1 here), ε is the asteroid's emissivity at the wavelength in question (also assumed to be 1 here), and σ is the Stefan-Boltzmann constant. Any point on the asteroid has a temperature that depends on its angle from the subsolar point (φ) as

$$T(\varphi) = T_0 \sqrt[4]{\cos(\varphi)} \tag{5}$$

Any point that is more than ninety degrees from the subsolar point is assumed to have a temperature of zero.

The fast-rotating model (FRM) assumes that the thermal emission from a given point balances the average solar flux (that is, averaged over a rotation period), so that the equator is the hottest part of the asteroid, and the temperature at any point depends only on its latitude. This is reasonable for a quickly rotating asteroid with high thermal inertia. The equatorial temperature is

$$T_{equ} = \sqrt[4]{\frac{(1-A)F}{\pi \varepsilon \sigma}} \tag{6}$$

The temperature at a latitude φ is then

$$T(\varphi) = T_{equ} \sqrt[4]{\cos(\varphi)} \tag{7}$$

In general, the fast-rotating model predicts less emission from any given point in the illuminated hemisphere, which therefore requires a larger asteroid to emit a given observed flux.

The thermal models allow for the determination of an asteroid's diameter and its Bond albedo. If its visual absolute magnitude (H) is also known, as it is for 2010 CN141, one can utilize the relation between absolute visual magnitude, diameter (D), and albedo to calculate its visual geometric albedo (p_v). From Harris and Lagerros (2002), the relation between the three is:

$$D = \frac{1329\,km}{\sqrt{p_v}} 10^{-H/5} \tag{8}$$

	STM value	STM uncertainty	FRM value	FRM uncertainty
Diameter	258 m	22 m	316 m	27 m
Bolometric Bond albedo	0.0119	0.0026	0.0079	0.0017
Visual geometric albedo	0.0303	0.0067	0.0201	0.0044

Table 1.– Physical properties of 2010 CN141, as derived from simple thermal models

The values do not agree within their uncertainties, since the given uncertainties are derived from only the stated uncertainties of the input parameters and do not account for potential errors in the thermal models' underlying assumptions. Note that 2010 CN141 is apparently quite dark, as the visual geometric albedo of asteroids is typically about 0.16.

Using the STM with the average flux from the May frames' bright spot yields a diameter of 239 ± 47 m; using the FRM gives 364 ± 71 m. These diameters, within their uncertainties, agree with the diameters derived with the corresponding model from the February observations.

	Final value	Random uncertainty	Systematic uncertainty
Diameter	287 m	18 m	29 m
Bolometric Bond albedo	0.0099	0.0016	0.0020
Visual geometric albedo	0.0252	0.0040	0.0051

Table 2.– Final values for properties of 2010 CN141, as determined from both models.

6. CONCLUSIONS

In February of 2010, WISE discovered 2010 CN141, a near-Earth asteroid with low albedo which therefore would be easy to miss in optical surveys. It was probably but not conclusively seen by WISE again in May 2010. It should be visible to ground-based observers in the fall of 2011. Thermal modeling indicates that 2010 CN141 has a diameter of about 290 meters. Considering its orbital geometry and assuming a typical density of 2 grams per cubic centimeter, if its orbit shifted and it impacted the Earth, it would release about 3000 TNT equivalent megatons, over fifty times more than the most powerful nuclear explosion. This is unlikely, but 2010 CN141 will nevertheless be monitored in the future.

7. ACKNOWLEDGMENTS

The author wishes to sincerely thank his mentor, Dr. Ned Wright, for his guidance throughout this project. Sara Petty and Sean Lake provided helpful advice on working with WISE data. Thanks are also due to the UCLA Department of Physics and Astronomy for providing technical and logistical support and for providing an excellent work environment. This project, completed as part of UCLA's Physics and Astronomy Research Experience for Undergraduates, was supported by grant NSF-PHY 0850501 from the National Science Foundation. WISE frames are processed and stored at the California Institute of Technology's Infrared Processing and Analysis Center. The WISE mission is funded by the National Aeronautics and Space Administration.

REFERENCES

Harris, A. W., and Lagerros, J. S. V. 2002. Asteroids in the Thermal Infrared. In: Bottke, W. F., Cellino, A., Paolicchi, P., Binzel, R. P. (Eds.), Asteroids III. Univ. of Arizona Press, Tucson, AZ, pp. 205-218.

Minor Planet Center. 2010a. Minor Planet Electronic Circular 2010-F91: Daily Orbit Update (2010 Mar. 29 UT). http://www.minorplanetcenter.org/mpec/K10/K10F91.html

Minor Planet Center. 2010b. Minor Planet Electronic Circular 2010-R24: Daily Orbit Update (2010 Sept. 4 UT). http://www.minorplanetcenter.org/mpec/K10/K10R24.html

Spahr, T. B. 2010. Minor Planet Electronic Circular 2010-D74: 2010 CN141. http://www.minorplanetcenter.org/mpec/K10/K10D74.html

Wright, E. L., Eisenhardt, P. R. M., Mainzer, A., Ressler, M. E., Cutri, R. M., Jarrett, T., Kirkpatrick, J. D., Padgett, D., McMillan, R. S., Skrutskie, M., Stanford, S. A., Cohen, M., Walker, R. G., Mather, J. C., Leisawitz, D., Gautier III, T. N., McLean, I., Benford, D., Lonsdale, C. J., Blain, A., Mendez, B., Irace, W. R., Duval, V., Liu, F., Royer, D., Heinrichsen, I., Howard, J., Shannon, M., Kendall, M., Walsh, A. L., Larsen, M., Cardon, J. G., Schick, S., Schwalm, M., Abid, M., Fabinsky, B., Naes, L., Tsai, C. 2010. The Wide-field Infrared Survey Explorer (WISE): Mission Description and Initial On-orbit Performance. Submitted to ApJ; currently available at http://arxiv.org/abs/1008.0031

Wright, E. L. 2010. Wide-Field Infrared Survey Explorer. http://www.astro.ucla.edu/~wright/WISE/

Yeomans, D. K. 2010. JPL Small-Body Database Browser: 2010 CN141. http://ssd.jpl.nasa.gov/sbdb.cgi?sstr=2010%20CN141